Am J Physiol Endocrinol Metab 299: E189–E197, 2010.
First published May 11, 2010; doi:10.1152/ajpendo.00516.2009.

Obese carboxypeptidase E knockout mice exhibit multiple defects in peptide hormone processing contributing to low bone mineral density

Niamh X. Cawley,[1]* Tulin Yanik,[1]* Alicja Woronowicz,[1] Weizhong Chang,[2] Joan C. Marini,[2] and Y. Peng Loh[1]

[1]*Section on Cellular Neurobiology, Program on Developmental Neuroscience,* [2]*Bone and Extracellular Matrix Branch, Eunice Kennedy Shriver National Institute of Child Health and Human Development, National Institutes of Health, Bethesda, Maryland*

Submitted 21 August 2009; accepted in final form 7 May 2010

Cawley NX, Yanik T, Woronowicz A, Chang W, Marini JC, Loh YP. Obese carboxypeptidase E knockout mice exhibit multiple defects in peptide hormone processing contributing to low bone mineral density. *Am J Physiol Endocrinol Metab* 299: E189–E197, 2010. First published May 11, 2010; doi:10.1152/ajpendo.00516.2009.—Carboxypeptidase E (CPE) is a prohormone/proneuropeptide processing enzyme, and mice bearing CPE mutations exhibit an obese and diabetic phenotype. Studies on CPE knockout (KO) mice revealed poor prohormone processing, resulting in deficiencies in peptide hormones/neuropeptides such as insulin, gonadotropin-releasing hormone, and cocaine- and amphetamine-regulated transcript (CART). Here, we show that CPE KO mice, an obese animal model, have low bone mineral density (BMD) accompanied by elevated plasma CTX-1 (carboxy-terminal collagen crosslinks), and osteocalcin, indicators of increased bone turnover. Receptor activator for NF-κB ligand (RANKL) expression was elevated ~2-fold relative to osteoprotegerin in the femur of KO animals, suggesting increased osteoclastic activity in the KO mice. In the hypothalamus, mature CART, a peptide involved in eating behavior and implicated in bone metabolism, was undetectable. The melanocortin and neuropeptide Y (NPY) systems in the hypothalamus have also been implicated in bone remodeling, since MC4R KO and NPY KO mice have increased BMD. However, reduction of α-MSH, the primary ligand of MC4R by up to 94% and the lack of detectable NPY in the hypothalamus of CPE KO do not recapitulate the single-gene KO phenotypes. This study highlights the complex physiological interplay between peptides involved in energy metabolism and bone formation and furthermore suggests the possibility that patients, bearing CPE and CART mutations leading to inactive forms of these molecules, may be at a higher risk of developing osteoporosis.

CARBOXYPEPTIDASE E (CPE) is a processing enzyme that is highly expressed in endocrine cells and peptidergic neurons (17, 19). It functions to cleave carboxy-terminally extended lysine and arginine residues from peptide hormone and neuropeptide intermediates to form bioactive peptides in the regulated secretory pathway (RSP). In addition to its enzymatic function, CPE has been shown to facilitate trafficking of several prohormones into the granules of the RSP (10, 26). Recently, live-cell imaging and coimmunoprecipitation studies demonstrated a role for its cytoplasmic carboxyl terminus in the transport of peptidergic vesicles via interaction with dynactin, an anterograde microtubule-based motor protein complex (27, 28). The involvement of CPE in multiple cellular functions would suggest that deficiencies in CPE would lead to many pathologies. Indeed, the CPE knockout (KO) mouse exhibits multiple endocrinopathies leading to diabetes, infertility, and obesity (7).

During our initial characterization of the phenotype of the CPE KO mice, which included physical and biochemical measurements as well as behavioral tests (7), we observed unexpectedly that bone mineral density (BMD) measurements of the CPE KO mice were lower than those of their wild-type (WT) littermate controls. This was somewhat unexpected (20), since increased weight imposed by an obesity phenotype, as in the case of the CPE KO mice, is correlated with increased BMD to counter the heavier load. BMD, as an indicator of bone structure, is modulated by two sequential cellular events, bone formation by osteoblasts and bone resorption by osteoclasts. The balance of the activity of these two cell types dictates the phenotype of the bone. Previously, it was shown that the regulation of bone remodeling is mediated centrally by leptin (13), a peptide hormone secreted by adipocytes in response to insulin (5). Leptin regulates bone resorption via the sympathetic nervous system (SNS) acting through the β_2-adrenergic receptor (33). The SNS favors bone resorption by increasing expression of the osteoclast differentiation factor, RANKL (receptor activator for NF-κB ligand), in osteoblast progenitor cells. In an opposing pathway, leptin also controls the expression of the hypothalamic neuropeptide, cocaine- and amphetamine-regulated transcript (CART). CART is expressed abundantly in the arcuate and paraventricular nuclei of the hypothalamus, where it acts on hypothalamic neurons as a potent anorexigenic peptide. In addition, CART exerts an inhibitory effect on bone resorption by blocking RANKL expression (13). As such the CART KO mouse has been reported to have reduced bone mass (13). Leptin also downregulates neuropeptide Y (NPY), a powerful orexigenic peptide in the hypothalamus that has also been reported to play a central role in bone regulation (3). Indeed, the NPY KO mouse as well as the NPY receptor KO (Y2 KO) mouse both result in increased bone formation (2, 3), demonstrating a significant role of NPY in bone resorption.

Another neural pathway that regulates bone remodeling is the POMC-melanocortin system, which also controls energy homeostasis, acting as a downstream regulator of leptin and insulin (9). MC4R is the predominant melanocortin receptor in the hypothalamus, and its primary ligand is α-MSH. Mice lacking MC4R (MC4R KO) have increased bone mass, a phenotype attributed to increased CART expression, since removing one allele of the *cart* gene from these KO mice normalized bone parameters without changing energy metabolism (1).

* N. X. Cawley and T. Yanik contributed equally as first authors.

Address for reprint requests and other correspondence: Y. P. Loh, National Institutes of Health, Bldg. 49, Rm 5A-22, 49 Convent Dr., Bethesda, MD 20892 (e-mail: lohp@mail.nih.gov).

 0193-1849/10 Copyright © 2010 the American Physiological Society

Downloaded from journals.physiology.org/journal/ajpendo at Orta Dogu Teknik Univ Kutuphanesi (144.122.007.037) on March 25, 2022.

Thus, several lines of evidence link the hormones involved in energy metabolism to bone remodeling. Here, we characterize several of these peptide hormones in the CPE KO mouse in an attempt to better evaluate the hierarchy of various peptidergic pathways, reported to be involved in bone remodeling, in one animal model. We show that CPE KO mice have low bone density and extremely low levels of α-MSH, NPY, and CART in the hypothalamus, resulting in an overall net increase in RANKL expression that causes an increase in osteoclasts and subsequent enhanced bone resorption.

MATERIALS AND METHODS

Animals. WT and CPE KO mice were housed in a secure animal facility at the National Institutes of Health, where they had access to regular chow and water ad libitum under a 12:12-h light-dark cycle. All procedures using the mice were in accordance with an animal protocol approved by the Animal Care and Use Committees (ACUC) of the National Institute of Child Health and Human Development.

Bone densitometry. A total of 32 mice (male CPE KO, $n = 8$, WT, $n = 8$; female CPE KO, $n = 8$, WT, $n = 8$) at 40–45 wk of age, were euthanized by cervical dislocation followed immediately by decapitation. The femoral and lumbar spine BMD (g/cm^2) was measured in the intact mouse with dual-energy X-ray absorptiometry (DEXA) using a GE Lunar PIXImus2 (Madison, WI) densitometer according to the manufacturer's instructions. The instrument was calibrated weekly using appropriate phantoms. The internal calibration standards were provided by GE. Precision error for BMD measurements was 2%-3% in the femoral regions. BMD values of CPE KO mouse femurs and lumbar spines were compared with those of age-matched, WT littermate controls.

Serum calcium, hormones, and bone marker analysis. Blood (~0.5–1 ml) was collected from deeply anesthetized CPE KO mice (3 males and 3 females, 35–45 wk of age) and their matching WT littermates by intracardiac puncture. Serum was separated from whole blood by centrifugation. Calcium, osteocalcin, PTH, corticosterone, and carboxy-terminal collagen crosslinks (CTX-1) values were analyzed under contract at Ani Lytics (Gaithersburg. MD). Osteocalcin was measured using a mouse Osteocalcin IRMA kit (ALPCO, Salem, NH), CTX-1 with the rat Laps Nordic Bioscience kit (Laps Nordic Biosciences, Herlev, Denmark), corticosterone using the MP Biomedicals ^{125}I-corticosterone kit (MP Biomedicals, Solon, OH), and PTH with an IRMA kit (ALPCO).

Immunoassay of α-MSH, CART, and NPY in hypothalmus or pituitary neurointermediate lobe. Dissected pituitary neurointermediate lobes (NILs) and hypothalami from WT and CPE KO mice were homogenized on ice with 100 μl of 0.1 M glacial acetic acid in the presence of an inhibitor cocktail (1× Complete; Boeringer, Mannheim, Germany) plus 1 mM NaF and 0.2 mM Na orthovanadate. The homogenates were heated at 95°C for 10 min and then centrifuged at 13,000 rpm for 20 min, and the supernatant was saved. The pellets were reextracted with 100 μl of the acid solution, and the resulting supernatant after centrifugation was added to the first supernatant and lyophilized. The samples were then reconstituted in 200 μl of RIA buffer and assayed for α-MSH by RIA using a kit from Phoenix Pharmaceuticals (Burlingame, CA). The samples from the hypothalami were also assayed by RIA for CART-IR (immunoreactivity) and by EIA for NPY-IR using kits from Phoenix Pharmaceuticals. CART-IR material was further analyzed by mass spectroscopy (see below), and NPY-IR material was analyzed by high-pressure liquid chromatography (HPLC) followed by EIA. The samples were separated by HPLC on a 4.6 × 250-mm 5-μm reverse-phase Jupiter C_{18} column (Phenomenex, Torrance, CA). The column was equilibrated in 40% *buffer B* (80% acetonitrile-20% methanol-0.1% TFA) and 60% *buffer A* (0.1% TFA) (29). The gradient went from 40% *buffer B* to 50% *buffer B* in 15 min. Eight fractions (nos. 7–14) were lyophilized and reconstituted in EIA buffer and assayed for authentic NPY. Two WT and two CPE KO mice were analyzed in this manner. Two micrograms of authentic NPY-amide standard (Phoenix Pharmaceuticals) was applied to the column and eluted in Fraction 10. The standard was monitored at 214 nm.

ProteinChip profiling analysis of CART-related molecules in hypothalamic extracts. Hypothalamic extracts from CPE KO and WT mice were analyzed for CART immunoreactive molecules using surface-enhanced laser desorption ionization time of flight mass spectroscopy (SELDI-TOF-MS) as described previously (7). Hypothalami were homogenized in 0.1 M HCl containing 1× protease inhibitors (Sigma, St. Louis, MO), and the cell debris was removed by centrifugation (5 min at 15,000 *g*). Anti-CART (55–102; Phoenix Pharmaceuticals), which recognizes the active forms of CART (COOH terminus of proCART), was coupled to the chips (PG20 ProteinChips) using the ProteinChip antibody capture kit (Ciphergen Biosystems, Freemont, CA). The chips were washed in PBS with 0.5% Triton X-100 and incubated with 1 μg of hypothalamic extract, after which they were washed and prepared for SELDI-TOF-MS. To facilitate desorption and ionization of the bound proteins on the ProteinChip array, 0.5 μl of matrix, cyano-4-hydroxycinnamic acid (Ciphergen Biosystems) in 50% acetonitrile containing 0.1% trifluoroacetic acid (TFA) was added to each spot on the chips and allowed to dry. The bound proteins on the chips were analyzed by SELDI using the Ciphergen ProteinChip reader. Negative control experiments (without antibodies or without serum) were run concurrently to control for experimental variations. All steps were performed at room temperature.

Western blot analysis of pituitary and hypothalamic tissue. The anterior lobe (AL) and neurointermediate lobe (NIL) of the pituitary and the hypothalamus from WT and CPE KO mice were dissected under a microscope. The tissues were collected and saved in Eppendorf tubes and homogenized on ice in 100 μl of lysis buffer (Tper lysis buffer, Pierce, IL) supplemented with 0.1% Triton X-100 and inhibitors (3× inhibitor cocktail; G-Biosciences, St. Louis, MO) using a plastic pestle. The samples were centrifuged at 13,000 rpm in a microfuge for 20 min, and the resulting supernatants were saved for analysis. Proteins from equivalent volumes of the lysates were separated by electrophoresis using minigels (12% Tris-glycine or 4–12% NuPage; Invitrogen, Piscataway, NJ) and then transferred to nitrocellulose or PVDF membranes. The pituitary blots were probed with rabbit anti-ACTH (DP4, 1:2,000, generated in our laboratory), which recognizes all forms of ACTH, including its precursor POMC and the 23-kDa POMC intermediates, and the hypothalamic blots were probed with mouse anti-MC4R (Santa Cruz Biotechnology, Santa Cruz, CA). Primary antibodies were detected by secondary anti-rabbit or anti-mouse antibodies coupled to an infrared fluorescent dye (IR-Dye 700 or 800; LI-COR Biosciences, Lincoln, NE). The signal was visualized on an Odyssey fluorescence detector (LI-COR Biosciences).

Serum levels of ACTH immunoreactive material. WT and CPE KO mice (age 36–40 wk) were euthanized by cervical dislocation followed by decapitation. Trunk blood was collected and the serum isolated by centrifugation and stored at −80°C until analyzed. Serum levels of POMC and 23-kDa POMC intermediates were assayed by ELISA using a kit (OCTEIA POMC) from Immunodiagnostic Systems (Tyne and Wear UK) that specifically detects only full-length POMC and the 23-kDa POMC intermediate. ACTH was assayed by a specific RIA using a kit (Phoenix Pharmaceuticals). To identify whether the ACTH in the sera of CPE KO mice was authentic ACTH, HPLC followed by RIA was used. Sera from 13 KO animals were combined and acidified with *buffer A* from the peptide extraction kit (Bachem) and the peptides purified through C_{18} cartridges. The eluate was lyophilized and reconstituted in 0.1% TFA. The peptides were then separated by HPLC on the same column described for NPY. The column was equilibrated in 40% *buffer B* (60% acetonitrile-0.1% TFA) and 60% *buffer A* (0.1% TFA). The gradient went from 40% *buffer B* to 70% *buffer B* in 30 min. All fractions were lyophilized,

Downloaded from journals.physiology.org/journal/ajpendo at Orta Dogu Teknik Univ Kutuphanesi (144.122.007.037) on March 25, 2022.

reconstituted in RIA buffer, and assayed for ACTH-IR material. Ten micrograms of authentic ACTH(1–39) was used as a standard (Bachem) and monitored at 214 nm. The standard eluted in fraction 17. Sera from 10 WT controls were treated identically and assayed in the same way.

Quantification of RANKL and osteoprotegerin expression. Total RNA was extracted from femurs of 6-mo-old WT and CPE KO mice (3 of each) using Tri Reagent (Molecular Research Center) treated with a DNA-Free Kit (DNase Treatment & Removal, Ambion). RNA integrity was verified by analysis on an Agilent 2100 Bioanalyzer. For real-time RT-PCR analysis, 5 μg of RNA was reverse transcribed using a High Capacity cDNA Archive Kit (Applied Biosystems) with random primers. TaqMan expression assays specific for the mRNA sequence of RANKL (Applied Biosystems, Mm00441908_m1) and osteoprotegerin (OPG; Applied Biosystems, Mm00435452_m1) were used for quantification of transcripts. RANKL and OPG expression levels were calculated using a control fibroblast mRNA standard curve and then normalized to GAPDH (Applied Biosystems, Mm99999915_g1).

Statistics. For all studies, P values were obtained using paired or unpaired two-tailed Student's t-tests.

RESULTS

Analysis of bone density in CPE KO mice. The bone densities of male and female 40- to 45-wk-old CPE KO mice and their WT littermates were evaluated by densitometry using DEXA scan. A representative scan of a CPE KO mouse is presented in Fig. 1*A*, showing the lumbar and femur areas where measurements were taken. The scans of the femur showed that both male and female WT mice had similar BMD values [0.091 ± 0.002 and 0.102 ± 0.008 g/cm^2, respectively (means ± SE), $n = 8$, $P = 0.25$]. Likewise, male and female CPE KO mice showed similar BMD values (0.083 ± 0.002 and 0.088 ± 0.003 g/cm^2, $n = 8$, $P = 0.23$), indicating no sex differences. BMD values from both males and females were therefore combined for analysis. Figure 1*B* shows that BMD in the femur was less in the CPE KO animals than in WT littermates ($n = 16$, 8 females and 8 males combined). BMD was 0.096 ± 0.004 g/cm^2 in the WT group ($n = 16$) and 0.085 ± 0.002 g/cm^2 in CPE KO animals ($n = 16$, $P = 0.012$). Similar results were obtained for the lumbar spine area (0.067 ± 0.005 and 0.053 ± 0.008 g/cm^2 in WT and CPE KO animals, respectively, $P < 0.05$).

Analysis of biochemical markers of bone turnover in CPE KO mice. To support the DEXA scan results indicating lower BMD in CPE KO mice, we carried out biochemical studies to measure serum levels of CTX-1 (a degradation product of type I collagen), a specific marker of bone resorption, and osteocalcin, a sensitive marker of bone formation secreted from osteoblasts. Table 1 shows that serum CTX-1 levels were significantly higher in the CPE KO animals, indicative of greater osteoclast activity and bone resorption in these mice compared with WT animals. Plasma levels of osteocalcin were also higher in the CPE KO mice relative to WT mice, suggestive of increased osteoblast activity. The higher levels of both CTX-1 and osteocalcin but lower BMD in CPE KO mice compared with WT animals indicates an overall higher bone turnover in the CPE KO animals but with an imbalance toward bone resorption. Serum Ca^{2+} levels in the CPE KO mice were somewhat elevated but did not reach statistical significance compared with WT mice (9.7 ng/ml for KO and 8.5 ng/ml for WT, $P = 0.076$; Table 1). Serum PTH and corticosterone were similar in both genotypes (Table 1).

Analysis of peptide hormones implicated in bone remodeling. Serum levels of leptin in the CPE KO mice were previously determined to be about four times higher than in their WT littermates (7).

CART: Analysis of CART-IR in the hypothalamus by RIA revealed an increase in total CART-IR in the CPE KO mice [87 ± 13 pg in WT ($n = 10$) vs. 132.8 ± 18.3 pg in CPE KO ($n = 5$) mice, $P = 0.023$]. This represents an increase of ~53% in the CPE KO mice hypothalami compared with WT (Fig. 2*A*). Analysis of these CART peptides using ProteinChip (SELDI-TOF-MS) antibody capture assay revealed incomplete processing of proCART to mature forms of CART (4.4 and 5.4 kDa) in the CPE KO mice (Fig. 2*B*). Additionally, higher levels of intermediate CART (6.1 kDa) and high molecular mass CART-IR (12 and 14.9 kDa) were detected in these mice compared with WT animals. This pattern of CART peptide forms is similar to that found in the circulation of CPE KO mice (7).

Neuropeptide Y: In the acid-extracted hypothalami, NPY-IR was not significantly different between WT and CPE KO animals [1.38 ± 0.45 ng/hypo ($n = 9$) in WT vs. 1.19 ± 0.24 ng/hypo ($n = 12$) in KO, $P = 0.69$; Fig. 3*A*]. However,

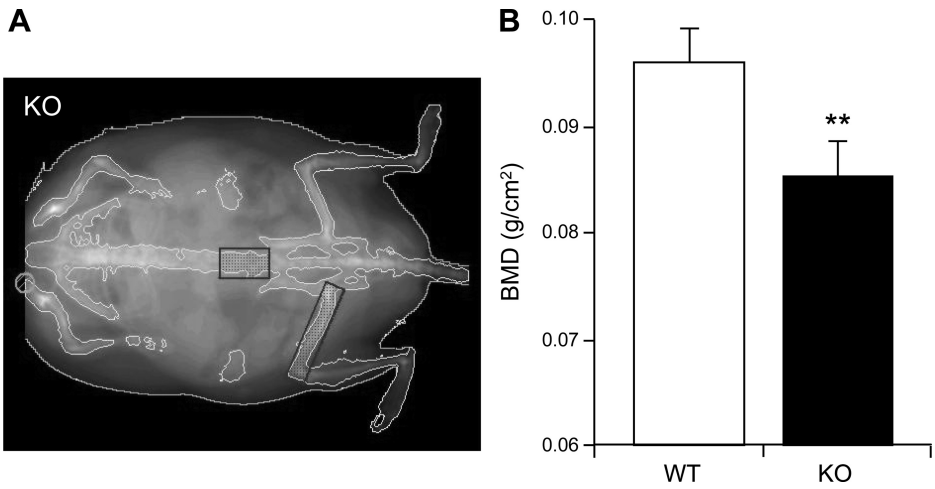

Fig. 1. *A*: representative DEXA scan of a carboxypeptidase E knockout (CPE KO) mouse. Boxed areas indicate femoral and lumbar areas where measurements were made. *B*: femoral bone mineral density (BMD, g/cm^2) in combined male and female WT and CPE KO mice. Bar graph shows DEXA scan BMD values of femur of CPE KO mice and their WT littermates; $n = 16$ mice/group. **$P < 0.01$.

Downloaded from journals.physiology.org/journal/ajpendo at Orta Dogu Teknik Univ Kutuphanesi (144.122.007.037) on March 25, 2022.

Table 1. *Serum levels of hormone and Ca^{2+} in WT and CPE KO mice*

Hormones and Ca^{2+}	Wild Type	CPE KO	*P* Value
Osteocalcin	41.7 ± 9.2 ng/ml	79.9 ± 17 ng/ml	0.01
CTX-1	21.0 ± 5.4 ng/ml	31.9 ± 8.0 ng/ml	0.01
Ca^{2+}	8.5 ± 1.5 mg/dl	9.7 ± 0.8 mg/dl	0.076
PTH	31.2 ± 11.4pg/ml	39.6 ± 13.3pg/ml	NS
Corticosterone	49.5 ± 7.0 ng/ml	70.7 ± 8.4 ng/ml	NS

Values are means ± SE; $n = 6$ for each genotype, except for corticosterone, $n = 3$. CPE, carboxypeptidase E; CTX-1, carboxy-terminal collagen crosslinks; PTH, parathyroid hormone; NS, not significant.

analysis by HPLC revealed that the NPY-IR did not include measurable amounts of authentic NPY-amide (Fig. 3*B*) and presumably represents higher molecular mass intermediates of proNPY.

α-MSH: Analysis of hypothalamic extracts showed a severe reduction in α-MSH [706.4 ± 96.4 ng/ml ($n = 10$) in WT vs. 43.1 ± 11.4 ng/ml ($n = 5$) in CPE KO mice, $P < 0.001$]. This represents a reduction of α-MSH in the CPE KO hypothalamus by 94% (Fig. 4*A*). Analysis of MC4R by Western blot demonstrated that similar levels of the receptor were present in hypothalami of WT and CPE KO mice (Fig. 4*B*).

ACTH: Western blot analysis of the AL showed that the levels of glycosylated and nonglycosylated mature ACTH forms (ACTH-IR) were significantly reduced in the CPE KO mice compared with WT (Fig. 5*A, left*). In the NIL of the pituitary, where α-MSH is the final processed product, we found that α-MSH was also severely reduced in the CPE-KO mice (Fig. 5*A, right*). Quantification of α-MSH by RIA showed a reduction of this peptide in the CPE KO mice [444.1 ± 69 ng/ml in WT ($n = 7$) vs. 85.3 ± 9.8 ng/ml in CPE KO ($n = 8$) mice, $P < 0.001$]. This represents a reduction of α-MSH in the CPE KO NIL by 81% (Fig. 5*B*). We also found that the levels of POMC and its 23-kDa biosynthetic intermediate in the NIL to be significantly higher in the CPE KO mice (Fig. 5*A, right*). This is in contrast to the AL, where the relative levels of POMC and the 23-kDa ACTH intermediate in both CPE KO

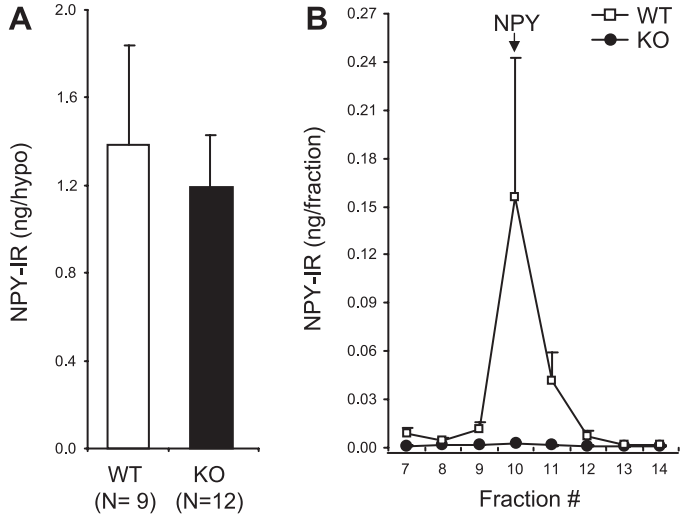

Fig. 3. *A*: ELISA of NPY-IR material in WT and CPE KO hypothalamic extracts. Bar graph shows that WT and CPE KO hypothalami contained similar levels of NPY-IR material. *B*: HPLC-EIA analysis of NPY-IR in hypothalamic extracts from 2 WT and 2 CPE KO mice. Peptides (see METHODS) were fractionated by reverse-phase HPLC and the fractions lyophilized, reconstituted in ELISA buffer, and analyzed by ELISA for NPY-IR. Values were averaged for both genotypes and graphed. Elution time for the synthetic peptide NPY-amide is indicated by the arrow. Note that authentic NPY-amide was readily detectable in WT extracts, whereas it was not detected in CPE KO extracts. This suggests that NPY-IR materials detected in *A* is likely to be unprocessed or intermediate forms of proNPY.

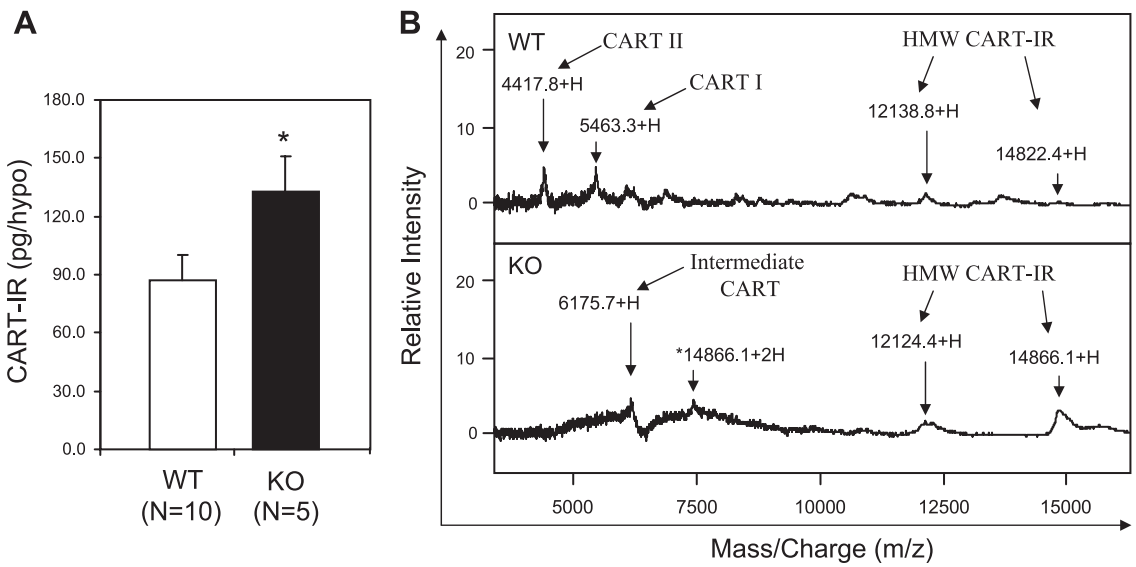

Fig. 2. *A*: RIA of cocaine- and amphetamine-regulated transcript (CART)-immunoreactive (IR) material in WT and CPE KO hypothalamic extracts. Bar graph shows that CPE KO hypothalami contained ~53% more CART-IR than WT. *$P < 0.05$. *B*: lack of bioactive CART in the hypothalamus of CPE KO mice. Surface-enhanced laser desorption ionization-time of flight mass spectrometry (SELDI-TOF-MS) chromatographic profiles of CART-IR peptides in hypothalami of WT and CPE KO male mice. Samples of hypothalamic extract from WT and CPE KO animals were analyzed using PG20 ProteinChips, which was coupled with anti-CART (55–102). Relative intensity (%) in mass/charge is plotted for each peptide and shown for the region between 0 and 15,000 Da. Active forms of CART: CART I (5.4 kDa), and CART II (4.4 kDa) were present in WT but not CPE KO mice. An intermediate form of CART (6.1 kDa) and high molecular mass forms (HMW) of CART-IR 12 and 14.9 kDa, consistent with posttranslationally modified proCART) were found in greater amounts in CPE KO than in WT animals. *Double-charged *m/z* peak of the 14.9-kDa HMW CART-IR peak.

Downloaded from journals.physiology.org/journal/ajpendo at Orta Dogu Teknik Univ Kutuphanesi (144.122.007.037) on March 25, 2022.

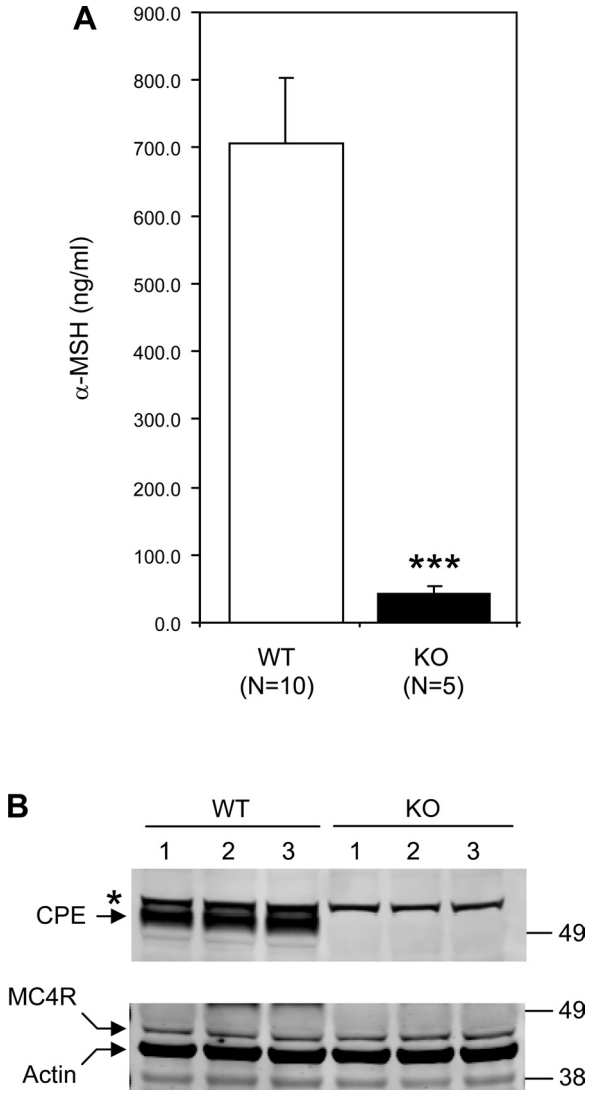

Fig. 4. *A*: RIA analysis of α-MSH in the hypothalamus of CPE KO and WT mice. Bar graph shows a 94% reduction of α-MSH in KO hypothalamic extracts. *B*: Western blot analysis of hypothalamic extracts for melanocortin 4 receptor (MC4R). Similar levels of MC4R were detected. β-Actin was immunostained and used to normalize for protein loading, and CPE was immunostained to confirm WT and KO phenotypes. *Represents a nonspecific band.

and WT animals were similar and suggest an upregulation of POMC synthesis in the NIL to compensate for the reduced α-MSH.

In the sera, levels of serum POMC and its biosynthetic intermediate (23-kDa ACTH) were about eight times higher in the CPE KO mice than in WT ($n = 11$ WT and $n = 12$ CPE KO; $P < 0.001$; Fig. 6*A*), whereas mature ACTH-IR levels in serum were not significantly different ($P = 0.089$, $n = 11$ for each group; Fig. 6*B*). Analysis of the ACTH-IR material by HPLC/RIA demonstrated that the levels and forms of ACTH-IR that included mature ACTH (4.5 kDa) were similar in the sera of both these genotypes (Fig. 7).

Analysis of RANKL and OPG expression in mouse femur. Real-time RT-PCR was carried out to quantify the levels of RANKL and OPG mRNA in femurs from WT and CPE KO mice. RANKL mRNA was increased about threefold in the KO femur compared with WT (WT, 1 ± 0.11 normalized units; KO, 2.89 ± 0.15 normalized units, $n = 3$, $P < 0.001$). OPG mRNA was also increased in the KO femur (WT, 1 ± 0.06 normalized units; KO, 1.46 ± 0.12 normalized units, $n = 3$, $P < 0.001$). The ratio of RANKL to OPG was increased about twofold in the KO femurs (WT, 1 ± 0.15 normalized units; KO, 1.98 ± 0.14 normalized units, $n = 3$, $P < 0.001$; Fig. 8), suggesting a net increase in signaling for osteoclastogenesis in CPE KO mice.

DISCUSSION

CPE is a single polypeptide protein whose original identification as an enzyme revealed only part of its function in physiology. We now know that CPE plays important roles in the synthesis, transport, processing, and secretion of many peptide hormones and neuropeptides. Hence, the CPE KO mouse represents an animal model whereby many pathological conditions resulting from the absence of CPE may be studied. While single gene deletions can be made in mice and the effect they have on a specific function within a specific tissue can be studied to provide insight into a disease state, the use of a single mouse model, as in the case of the CPE KO mouse, to study multiple conditions is an exciting albeit complex prospect. We initially characterized the CPE KO mouse with respect to its most obvious phenotypes: obesity, diabetes, and infertility (7). Other studies on CPE KO mice have shown defective secretion of mature brain-derived neurotrophic factor (BDNF) in the hippocampus (26), defective secretion of glutamate in the retina (40), specific neuronal degeneration in the CA3 region of the hippocampus (36), and defective dendritic pruning and spine formation of layer V cortical neurons (6, 35). Thus CPE appears to play a role, either directly or indirectly, in many processes both inside and outside the central nervous system.

CPE KO mice develop obesity such that adult mice can have more than 50% of their weight contributed by fat. Contributing factors to this phenotype are hyperphagic behavior, decreased fat utilization, lower metabolism, and reduced activity (7). As part of our initial characterization, we noticed that these obese mice have lower BMD (Fig. 1). Elevated levels of CTX-1 and osteocalcin, both markers of bone turnover (Table 1), suggest that bone metabolism was increased, with a possible imbalance toward bone resorption. We also determined the levels of PTH and corticosterone in the serum and found that they were not significantly different from WT animals, suggesting that these molecules and their signaling pathways are not responsible for the decreased BMD in the CPE KO mice.

Bone turnover is the balance between resorption by osteoclasts and formation by osteoblasts. This balance is primarily governed by the expression levels of RANKL (24) and its soluble decoy OPG (31). RANKL activates osteoblast progenitors to differentiate into osteoclasts, whereas OPG acts as a binding protein to RANKL, effectively regulating its activity. In the femurs of CPE KO mice, we found that both RANKL and OPG expression levels are increased; however, the RANKL/OPG ratio is increased twofold in KO animals compared with WT littermates (Fig. 8), suggesting that the decreased BMD is likely due to increased osteoclast activity. Indeed, our preliminary histomorphometry studies indicate that there are 60% more osteoclasts in the femur of CPE KO than

Downloaded from journals.physiology.org/journal/ajpendo at Orta Dogu Teknik Univ Kutuphanesi (144.122.007.037) on March 25, 2022.

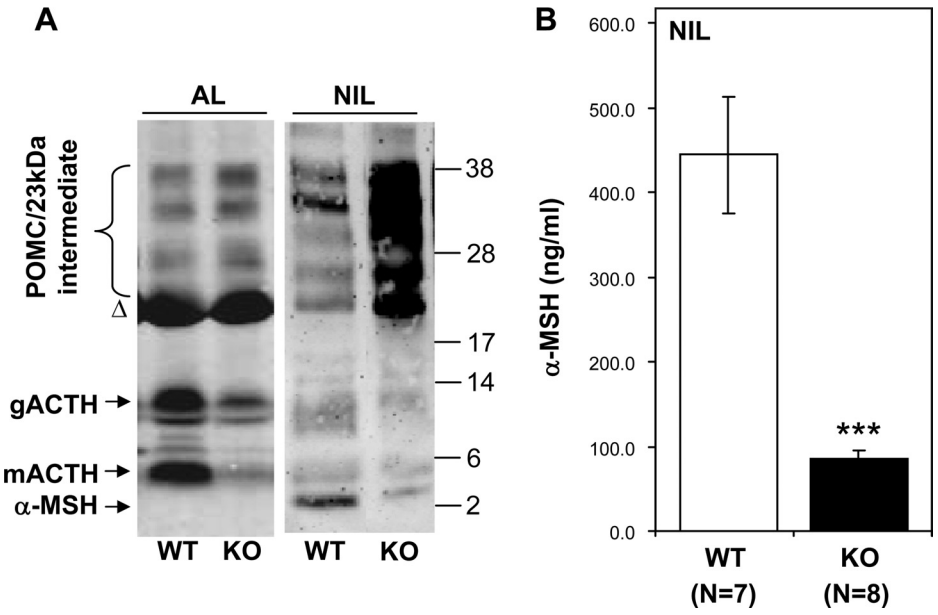

Fig. 5. *A*: Western blot analysis of anterior lobe (AL) and neurointermediate lobe (NIL) of the pituitary of WT and CPE KO mice for ACTH-IR material. In AL, glycosylated ACTH (gACTH, ~13 kDa) and mature ACTH (mACTH, ~4.5 kDa) and in NIL, α-MSH levels were significantly reduced in CPE KO mice. Note increased levels of proopiomelanocortin (POMC) and its biosynthetic intermediates in the NIL lane from CPE KO mice. Δ, nonspecific staining of growth hormone. *B*: RIA analysis of α-MSH in NIL of CPE KO and WT mice. Bar graph shows 81% reduction of α-MSH in KO NIL extracts.

in WT mice, whereas osteoblast numbers were similar (data not shown).

It has recently been shown that leptin itself functions in bone regulation through activation of the SNS to upregulate RANKL expression and is independent of its role in the regulation of energy metabolism (30). Leptin also increases the expression of CART, which inhibits RANKL expression (13). CART is expressed predominantly in the hypothalamus, where it acts as an anorexigenic peptide on hypothalamic neurons. It is also expressed to a much lesser extent in pituitary, adrenal glands (23), islets of Langerhans (21), and gut (12). As expected for such a peptide, CART KO mice and humans with mutations in the CART gene (11) develop obesity presumably due to hyperphagic behavior. However, the CART KO mice have conflicting reports as to whether bone regulation is affected (4, 13, 32). Since serum leptin levels are approximately fourfold higher in these obese CPE KO mice (7), leptin signaling via the SNS may contribute to the increase in bone resorption in these mice. The SNS appears to be functioning normally in the CPE KO mice, since signaling to brown adipose tissue appears normal because levels of uncoupling protein-1 are similar in WT and KO animals (data not shown). Significantly elevated leptin levels in the CPE KO mice would also be expected to increase bone mass through increased hypothalamic CART expression (13). Our results show that, indeed, total CART-IR levels are increased compared with WT mice (Fig. 2*A*), but it is not processed to mature CART (Fig. 2*B*). This would lead to favored signaling of the SNS compared with CART signaling resulting in bone resorption.

Other peptide hormones such as α-MSH and NPY have been shown to contribute to bone morphology. The loss of α-MSH

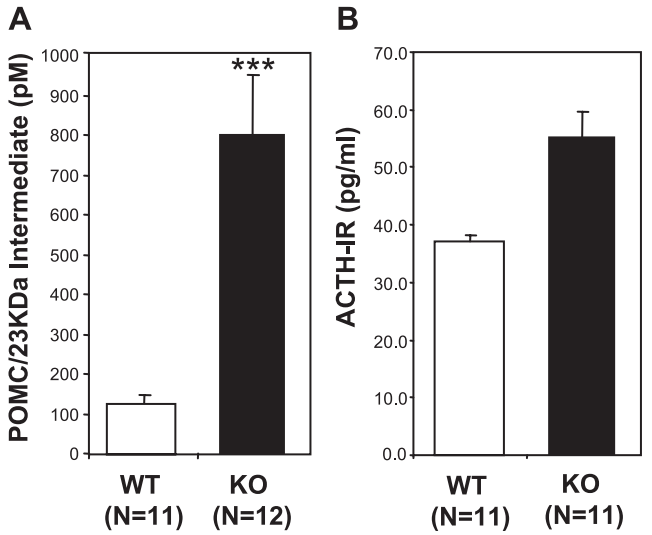

Fig. 6. *A*: ELISA analysis of serum from WT and CPE KO mice specifically for full-length POMC and its biosynthetic intermediates. Bar graph shows 8 times as much POMC/intermediate in sera from CPE KO mice compared with WT, ***$P < 0.001$. *B*: RIA analysis of WT and CPE KO serum for ACTH-IR. Bar graph shows a slight but nonsignificant increase in ACTH-IR in sera from CPE KO mice.

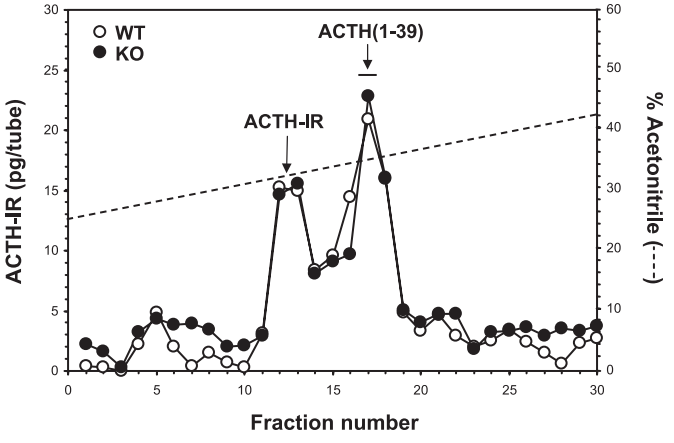

Fig. 7. HPLC-RIA analysis of ACTH-IR in serum from WT and CPE KO mice. Peptides extracted from pooled sera from 10 WT and 13 CPE KO mice were fractionated by RP-HPLC. Fractions were lyophilized, reconstituted in RIA buffer, and analyzed by RIA for ACTH immunoreactivity. Elution time for the synthetic peptide ACTH(1–39) is indicated with an arrow. Note that levels and forms of ACTH-IR appear to be identical between WT and CPE KO mouse sera.

Downloaded from journals.physiology.org/journal/ajpendo at Orta Dogu Teknik Univ Kutuphanesi (144.122.007.037) on March 25, 2022.

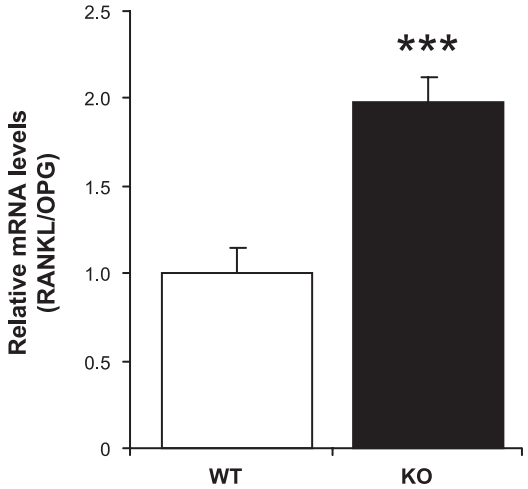

Fig. 8. Quantitative real-time PCR for mRNA levels of receptor activator for NF-κB ligand (RANKL) and osteoprotegerin (OPG) in femur extracts of WT and CPE KO mice. The ratio of RANKL to OPG levels is 2 times higher in CPE KO mice than in WT ($n = 3$ for each), indicative of a signaling pathway leading to osteoclastogenesis. ***$P < 0.001$.

signaling in the MC4R KO mice or the loss of signaling of NPY in the NPY KO or Y2 KO mice both result in increased bone formation. Levels of α-MSH in the hypothalamus and IL are severely diminished in the CPE KO mice (Figs. 4 and 5), as are the levels of NPY in the hypothalamus (Fig. 3). It is expected that, with such a reduction of these peptides in general, the phenotype of these mice should approach one with high BMD, similar to that of the KO mice mentioned above. However, the CPE KO mice showed low BMD in contrast to what would be expected, suggesting that α-MSH and NPY may play a less significant role in bone remodeling than CART. Indeed, in the MC4R KO mice the phenotype was attributed to increased levels of CART production (1). Hence, α-MSH appears to be upstream of CART in its role in bone regulation.

ACTH has been reported to be capable of inducing osteoblast proliferation (15, 39). In addition, all five melanocortin receptors are expressed on osteoblasts (39). Hence, the role of ACTH (or lack thereof) in the maintenance of osteoblast numbers might be a contributing factor in the decreased BMD of the KO mice. This turned out not to be the case, since circulating levels of ACTH appeared to be normal (Fig. 7). These analyses, corroborated by the normal levels of corticosterone (Table 1), however, have presented us with a puzzle that deserves attention. Circulating ACTH is normally secreted by corticotrophs of the AL in response to corticotropin-releasing factor (CRF) from the hypothalamus. Our analysis of the AL shows severely reduced levels of ACTH in this tissue and is therefore unlikely to be the primary source of the circulating ACTH. We speculate that the source of the circulating ACTH is from the IL of the pituitary, based on the observations that, through compensation for the lack of production of α-MSH in the IL, POMC and its processing intermediates are greatly increased (Fig. 5*A*). This increase provides sufficient substrate for the low level of processing that is present, presumably by carboxypeptidase D, to obtain sufficient levels of ACTH that get secreted. The RSP of the IL is under tonic inhibition by dopamine from the hypothalamus. In light of recent findings that CPE plays a role in the trafficking of the dopamine transporter (38), defects in dopamine signaling, resulting in reduced inhibition of the RSP, would result in elevated basal secretion. This would also explain the source of the approximately eightfold elevation in levels of the POMC/23-kDa intermediate detected in the sera (Fig. 6*A*).

The increased serum level of osteocalcin in the CPE KO mice compared with WT littermates is interesting. Since osteocalcin acts on the pancreas to stimulate insulin secretion (25), and on fat cells to enhance secretion of adiponectin to increase insulin sensitivity (16), the high levels of osteocalcin secreted may be a physiological response to the diabetic state of the CPE KO animals (7), providing another pathway to facilitate maintenance of blood glucose homeostasis. Thus, osteocalcin may be particularly important in regulating insulin and adiponectin secretion in diabetic animals.

In conclusion, the obese CPE KO mice have low BMD due to an increase in osteoclast activity from increased RANKL expression driven by the SNS. The inability of the CPE KO mice to generate mature CART results in an inability to counterbalance the effect of the SNS by reducing RANKL expression. Furthermore, although the signaling of α-MSH and NPY each plays a role in regulating bone morphology, in the context of the CPE KO mouse the expected phenotypes are superseded by the lack of mature CART, further supporting other studies that CART is an important player associated with regulating bone remodeling. Our study also suggests that patients lacking mature

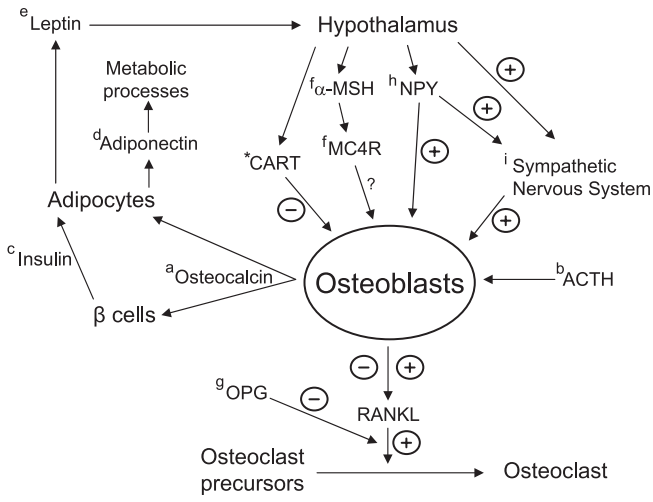

Fig. 9. Schema representing some of the complexity involved in the interplay between peptides from hypothalamus (CART, NPY, α-MSH), adipocytes (leptin), and osteoblasts (osteocalcin) and the SNS to maintain regulation of bone remodeling. +, signaling in favor of osteoclastogenesis; −, signaling that prevents it. [a]Osteocalcin is released from osteoblasts and activates the pancreatic β-cell to release insulin and the adipocyte to release adiponectin (16, 25). [b]ACTH plays a role in ostoblast proliferation (15, 39). [c]Insulin acts on the adipocyte to release leptin (5). [d]Adiponectin affects metabolic processes including insulin sensitivity (18). [e]Leptin activates the hypothalamus to express anorxigenic peptides α-MSH and CART and decrease orexigenic peptides NPY and AgRP as well as to stimulate the SNS (13, 14). [f]MC4R signaling is involved in bone metabolism presumably through elevation of CART expression (1). [g]Osteoprotegerin regulates osteoblast differentiation (24). [h]NPY plays a central role in bone remodeling (2). [i]SNS regulates bone remodeling (33). *Reduced CART levels are associated with poor bone mineral density and are downstream of α-MSH and NPY's role in bone metabolism (this study).

Downloaded from journals.physiology.org/journal/ajpendo at Orta Dogu Teknik Univ Kutuphanesi (144.122.007.037) on March 25, 2022.

CART, such as those bearing the Leu34Phe mutation in the *Cart* gene (37) that are hyperphagic and obese might also have poor BMD and raises the possibility that patients bearing CPE mutations (8) may have defects in bone regulation. Thus, the CPE KO mouse could serve as a model for understanding the pathophysiology of humans bearing mutations in the CPE (8, 22, 34) and the CART gene (11), who lack bioactive forms of these molecules. Finally, our findings indicate important interplay among the central nervous system and pituitary neuropeptides CART, NPY, and α-MSH, adipocyte leptin, and osteocalcin from osteoblasts in regulating bone remodeling and energy metabolism (Fig. 9).

ACKNOWLEDGMENTS

We thank Dr. Thomas Uveges from the Marini laboratory for help with the DEXA scan. We also thank Dr. Julia Barsony (Georgetown University) for helpful discussions about the manuscript.

Current address of T. Yanik: Dept. of Biological Sciences, Middle East Technical University, Ankara, Turkey.

GRANTS

This research was supported by the Intramural Research Program of the Eunice Kennedy Shriver National Institute of Child Health and Human Development, National Institutes of Health, Bethesda, MD.

DISCLOSURES

No conflicts of interest are reported by the authors.

REFERENCES

1. **Ahn JD, Dubern B, Lubrano-Berthelier C, Clement K, Karsenty G.** Cart overexpression is the only identifiable cause of high bone mass in melanocortin 4 receptor deficiency. *Endocrinology* 147: 3196–3202, 2006.
2. **Baldock PA, Lee NJ, Driessler F, Lin S, Allison S, Stehrer B, Lin EJ, Zhang L, Enriquez RF, Wong IP, McDonald MM, During M, Pierroz DD, Slack K, Shi YC, Yulyaningsih E, Aljanova A, Little DG, Ferrari SL, Sainsbury A, Eisman JA, Herzog H.** Neuropeptide Y knockout mice reveal a central role of NPY in the coordination of bone mass to body weight. *PLoS One* 4: e8415, 2009.
3. **Baldock PA, Sainsbury A, Couzens M, Enriquez RF, Thomas GP, Gardiner EM, Herzog H.** Hypothalamic Y2 receptors regulate bone formation. *J Clin Invest* 109: 915–921, 2002.
4. **Bartell SM, Isales CM, Baile CA, Kuhar MJ, Hamrick MW.** CART deficiency increases body weight but does not alter bone strength. *J Musculoskelet Neuronal Interact* 8: 146–153, 2008.
5. **Cammisotto PG, Bukowiecki LJ.** Mechanisms of leptin secretion from white adipocytes. *Am J Physiol Cell Physiol* 283: C244–C250, 2002.
6. **Carrel D, Du Y, Komlos D, Hadzimichalis NM, Kwon M, Wang B, Brzustowicz LM, Firestein BL.** NOS1AP regulates dendrite patterning of hippocampal neurons through a carboxypeptidase E-mediated pathway. *J Neurosci* 29: 8248–8258, 2009.
7. **Cawley NX, Zhou J, Hill JM, Abebe D, Romboz S, Yanik T, Rodriguiz RM, Wetsel WC, Loh YP.** The carboxypeptidase E knockout mouse exhibits endocrinological and behavioral deficits. *Endocrinology* 145: 5807–5819, 2004.
8. **Chen H, Jawahar S, Qian Y, Duong Q, Chan G, Parker A, Meyer JM, Moore KJ, Chayen S, Gross DJ, Glaser B, Permutt MA, Fricker LD.** Missense polymorphism in the human carboxypeptidase E gene alters enzymatic activity. *Hum Mutat* 18: 120–131, 2001.
9. **Cone RD.** The central melanocortin system and energy homeostasis. *Trends Endocrinol Metab* 10: 211–216, 1999.
10. **Cool DR, Normant E, Shen F, Chen HC, Pannell L, Zhang Y, Loh YP.** Carboxypeptidase E is a regulated secretory pathway sorting receptor: genetic obliteration leads to endocrine disorders in Cpe(fat) mice. *Cell* 88: 73–83, 1997.
11. **del Giudice EM, Santoro N, Cirillo G, D'Urso L, Di Toro R, Perrone L.** Mutational screening of the CART gene in obese children: identifying a mutation (Leu34Phe) associated with reduced resting energy expenditure and cosegregating with obesity phenotype in a large family. *Diabetes* 50: 2157–2160, 2001.
12. **Ekblad E.** CART in the enteric nervous system. *Peptides* 27: 2024–2030, 2006.
13. **Elefteriou F, Ahn JD, Takeda S, Starbuck M, Yang X, Liu X, Kondo H, Richards WG, Bannon TW, Noda M, Clement K, Vaisse C, Karsenty G.** Leptin regulation of bone resorption by the sympathetic nervous system and CART. *Nature* 434: 514–520, 2005.
14. **Elefteriou F, Takeda S, Ebihara K, Magre J, Patano N, Kim CA, Ogawa Y, Liu X, Ware SM, Craigen WJ, Robert JJ, Vinson C, Nakao K, Capeau J, Karsenty G.** Serum leptin level is a regulator of bone mass. *Proc Natl Acad Sci USA* 101: 3258–3263, 2004.
15. **Evans JF, Niu QT, Canas JA, Shen CL, Aloia JF, Yeh JK.** ACTH enhances chondrogenesis in multipotential progenitor cells and matrix production in chondrocytes. *Bone* 35: 96–107, 2004.
16. **Ferron M, Hinoi E, Karsenty G, Ducy P.** Osteocalcin differentially regulates beta cell and adipocyte gene expression and affects the development of metabolic diseases in wild-type mice. *Proc Natl Acad Sci USA* 105: 5266–5270, 2008.
17. **Fricker LD, Snyder SH.** Enkephalin convertase: purification and characterization of a specific enkephalin-synthesizing carboxypeptidase localized to adrenal chromaffin granules. *Proc Natl Acad Sci USA* 79: 3886–3890, 1982.
18. **Fu Y, Luo N, Klein RL, Garvey WT.** Adiponectin promotes adipocyte differentiation, insulin sensitivity, and lipid accumulation. *J Lipid Res* 46: 1369–1379, 2005.
19. **Hook VY, Loh YP.** Carboxypeptidase B-like converting enzyme activity in secretory granules of rat pituitary. *Proc Natl Acad Sci USA* 81: 2776–2780, 1984.
20. **Huszar D, Lynch CA, Fairchild-Huntress V, Dunmore JH, Fang Q, Berkemeier LR, Gu W, Kesterson RA, Boston BA, Cone RD, Smith FJ, Campfield LA, Burn P, Lee F.** Targeted disruption of the melanocortin-4 receptor results in obesity in mice. *Cell* 88: 131–141, 1997.
21. **Jensen PB, Kristensen P, Clausen JT, Judge ME, Hastrup S, Thim L, Wulff BS, Foged C, Jensen J, Holst JJ, Madsen OD.** The hypothalamic satiety peptide CART is expressed in anorectic and non-anorectic pancreatic islet tumors and in the normal islet of Langerhans. *FEBS Lett* 447: 139–143, 1999.
22. **Jia EZ, Wang J, Yang ZJ, Zhu TB, Wang LS, Wang H, Li CJ, Chen B, Cao KJ, Huang J, Ma WZ.** Association of the mutation for the human carboxypeptidase E gene exon 4 with the severity of coronary artery atherosclerosis. *Mol Biol Rep* 36: 245–254, 2009.
23. **Koylu EO, Couceyro PR, Lambert PD, Ling NC, DeSouza EB, Kuhar MJ.** Immunohistochemical localization of novel CART peptides in rat hypothalamus, pituitary and adrenal gland. *J Neuroendocrinol* 9: 823–833, 1997.
24. **Lacey DL, Timms E, Tan HL, Kelley MJ, Dunstan CR, Burgess T, Elliott R, Colombero A, Elliott G, Scully S, Hsu H, Sullivan J, Hawkins N, Davy E, Capparelli C, Eli A, Qian YX, Kaufman S, Sarosi I, Shalhoub V, Senaldi G, Guo J, Delaney J, Boyle WJ.** Osteoprotegerin ligand is a cytokine that regulates osteoclast differentiation and activation. *Cell* 93: 165–176, 1998.
25. **Lee NK, Karsenty G.** Reciprocal regulation of bone and energy metabolism. *Trends Endocrinol Metab* 19: 161–166, 2008.
26. **Lou H, Kim SK, Zaitsev E, Snell CR, Lu B, Loh YP.** Sorting and activity-dependent secretion of BDNF require interaction of a specific motif with the sorting receptor carboxypeptidase E. *Neuron* 45: 245–255, 2005.
27. **Park JJ, Cawley NX, Loh YP.** A bi-directional carboxypeptidase E-driven transport mechanism controls BDNF vesicle homeostasis in hippocampal neurons. *Mol Cell Neurosci* 39: 63–73, 2008.
28. **Park JJ, Cawley NX, Loh YP.** Carboxypeptidase E cytoplasmic tail-driven vesicle transport is key for activity-dependent secretion of peptide hormones. *Mol Endocrinol* 22: 989–1005, 2008.
29. **Schoofs L, Danger JM, Jegou S, Pelletier G, Huybrechts R, Vaudry H, De Loof A.** NPY-like peptides occur in the nervous system and midgut of the migratory locust, Locusta migratoria, and in the brain of the grey fleshfly, Sarcophaga bullata. *Peptides* 9: 1027–1036, 1988.
30. **Shi Y, Yadav VK, Suda N, Liu XS, Guo XE, Myers MG Jr, Karsenty G.** Dissociation of the neuronal regulation of bone mass and energy metabolism by leptin in vivo. *Proc Natl Acad Sci USA* 105: 20529–20533, 2008.
31. **Simonet WS, Lacey DL, Dunstan CR, Kelley M, Chang MS, Luthy R, Nguyen HQ, Wooden S, Bennett L, Boone T, Shimamoto G, DeRose**

Downloaded from journals.physiology.org/journal/ajpendo at Orta Dogu Teknik Univ Kutuphanesi (144.122.007.037) on March 25, 2022.

M, Elliott R, Colombero A, Tan HL, Trail G, Sullivan J, Davy E, Bucay N, Renshaw-Gegg L, Hughes TM, Hill D, Pattison W, Campbell P, Sander S, Van G, Tarpley J, Derby P, Lee R, Boyle WJ. Osteoprotegerin: a novel secreted protein involved in the regulation of bone density. *Cell* 89: 309–319, 1997.

32. **Singh MK, Elefteriou F, Karsenty G.** Cocaine- and amphetamine-regulated transcript may regulate bone remodeling as a circulating molecule. *Endocrinology* 149: 3933–3941, 2008.
33. **Takeda S, Elefteriou F, Levasseur R, Liu X, Zhao L, Parker KL, Armstrong D, Ducy P, Karsenty G.** Leptin regulates bone formation via the sympathetic nervous system. *Cell* 111: 305–317, 2002.
34. **Utsunomiya N, Ohagi S, Sanke T, Tatsuta H, Hanabusa T, Nanjo K.** Organization of the human carboxypeptidase E gene and molecular scanning for mutations in Japanese subjects with NIDDM or obesity. *Diabetologia* 41: 701–705, 1998.
35. **Woronowicz A, Cawley NX, Chang SY, Koshimizu H, Phillips AW, Xiong ZG, Loh YP.** Carboxypeptidase E knockout mice exhibit abnormal dendritic arborization and spine morphology in central nervous system neurons. *J Neurosci Res* 88: 64–72, 2010.
36. **Woronowicz A, Koshimizu H, Chang SY, Cawley NX, Hill JM, Rodriguiz RM, Abebe D, Dorfman C, Senatorov V, Zhou A, Xiong ZG, Wetsel WC, Loh YP.** Absence of carboxypeptidase E leads to adult hippocampal neuronal degeneration and memory deficits. *Hippocampus* 18: 1051–1063, 2008.
37. **Yanik T, Dominguez G, Kuhar MJ, Del Giudice EM, Loh YP.** The Leu34Phe ProCART mutation leads to cocaine- and amphetamine-regulated transcript (CART) deficiency: a possible cause for obesity in humans. *Endocrinology* 147: 39–43, 2006.
38. **Zhang H, Li S, Wang M, Vukusic B, Pristupa ZB, Liu F.** Regulation of dopamine transporter activity by carboxypeptidase E. *Mol Brain* 2: 10, 2009.
39. **Zhong Q, Sridhar S, Ruan L, Ding KH, Xie D, Insogna K, Kang B, Xu J, Bollag RJ, Isales CM.** Multiple melanocortin receptors are expressed in bone cells. *Bone* 36: 820–831, 2005.
40. **Zhu X, Wu K, Rife L, Cawley NX, Brown B, Adams T, Teofilo K, Lillo C, Williams DS, Loh YP, Craft CM.** Carboxypeptidase E is required for normal synaptic transmission from photoreceptors to the inner retina. *J Neurochem* 95: 1351–1362, 2005.

Downloaded from journals.physiology.org/journal/ajpendo at Orta Dogu Teknik Univ Kutuphanesi (144.122.007.037) on March 25, 2022.